ISBN: 978-3-95450-232-5 ISSN: 2673-7000 doi:10.18429/JACoW-NAPAC2022-TUZE4

PARTICLE-IN-CELL SIMULATIONS OF HIGH CURRENT DENSITY ELECTRON BEAMS IN THE SCORPIUS LINEAR INDUCTION ACCELERATOR*

S. E. Clark†, W. D. Stem, C. N. Melton, A. Fetterman, Y.-J. Chen, J. Ellsworth
Lawrence Livermore National Laboratory, 7000 East Ave., Livermore, CA 94550, USA

Abstract

Particle-in-cell (PIC) simulations of a high current density (I > 1 kA), and highly relativistic electron beam (E ~ 2-20 MeV) in the Scorpius Linear Induction Accelerator (LIA) are presented. The simulation set consists of a 3D electrostatic/magnetostatic simulation coupled to a 2D XY slice solver that propagates the beam through the proposed accelerator lattice for Scorpius, a next-generation flash X-ray radiography source. These simulations focus on the growth of azimuthal modes in the beam (e.g. Diocotron instability) that arise when physical ring distributions manifest in the beam either due to electron optics or solenoidal focusing and transport. The saturation mechanism appears to lead to the generation of halo particles and conversion down to lower mode numbers as the width of the ring distribution increases. The mode growth and saturation can contribute to the generation of hot spots on the target as well possible azimuthal asymmetries in the radiograph. Simulation results are compared to linear theory and tuning parameters are investigated to mitigate the growth of azimuthal modes in the Scorpius electron beam.

INTRODUCTION

Flash X-Ray Radiography has been used in the United States and around the world for many years as a diagnostic tool for imaging highly kinetic experiments. Hydrodynamic testing facilities such as the Lawrence Livermore National Laboratory (LLNL) Flash X-Ray (FXR) Linear Induction Accelerator (LIA) [1-4] and the Los Alamos National Laboratory (LANL) Dual-Axis Radiographic Hydrodynamic Test Facility (DARHT/DARHT-II) [5-6] have been developed and operated for many years. The Scorpius LIA has been conceived to improve the performance characteristics of the accelerator power systems by driving the accelerator with solid state pulsed power (SSPP). [7] This allows the pulses to be modulated to improve inter-pulse spacing, pulse rise times, energy variation, and current variation. These improvements in the pulse quality translate to superior multi-pulse radiographic performance by generating a sharper and flatter high voltage pulse. There is existing simulation work on DARHT-II in the injector [8] and the accelerator [9] which have focused on analysing component misalignment and instability growth. There also exists work for Scorpius to simulate the electron beam from cathode to target [10-11] using simulation tools like Trak, XTR, and LSP-slice.

This paper will focus assessing the impact of having non-monotonically decreasing beam density profile, which can lead to growth of the Diocotron instability. A 2D particle-in-cell (PIC) slice code will be used in conjunction with the 3D PIC code used in the diode (AK) gap region [12] of the injector to analyse the emittance growth of the beam throughout the accelerator. An updated Warp XY-slice solver was developed to model the accelerator gaps and the beam self-fields in the highly relativistic limit. This paper will discuss the analytical diocotron growth rate and how it compares to simulations of the Scorpius beamline. It will be shown that while there is diocotron instability growth, the observed emittance growth is tolerable in the Scorpius beamline.

ANALYTICAL GROWTH RATE FOR A NOMINAL HOLLOW BEAM

There has been much analysis of diocotron instability in one component plasmas, e.g. Penning-Malmberg traps [13-15] and in relativistic electron beams [16], which demonstrates that 2D particle-in-cell codes are well suited to modelling this phenomenon and that the growth rates match fairly well in the linear regime. The growth rate has been found to be $\gamma_D \propto \frac{\Omega_D}{2\gamma^2}$, where $\Omega_D = \omega_{pe}^2/\omega_{ce}$, γ_D is the characteristic growth rate for an e-fold, ω_{pe} is the electron plasma frequency, ω_{ce} is the electron cyclotron frequency, and γ is the relativistic gamma. The analytical growth rate for a hollow core beam with uniform density in an annulus is expressed as:

$$\gamma_D(l) = \frac{\Omega_D}{2\gamma^2}\left\{4\left(\frac{b}{d}\right)^{2l}\left[1 - l\left(1 - \left(\frac{b}{d}\right)^2\right)\left(\frac{d}{R}\right)^{2l}\right] - \left[2 - l\left(1 - \left(\frac{b}{d}\right)^2\right) - \left(\frac{d}{R}\right)^{2l}\left(1 - \left(\frac{b}{d}\right)^{2l}\right)\right]^2\right\}^{\frac{1}{2}}, \quad (1)$$

where R is the radius of the conducting wall, b is the inner radius of the beam annulus, and d is the outer radius of the beam annulus. It should be noted that in the highly relativistic case, the growth rate is divided by γ^2 to account for the self-generated beam magnetic fields.

Figure 1 shows the computed growth rates for one instance of beam radius. When examining different beam

*This work was performed under the auspices of the U.S. Department of Energy by Lawrence Livermore National Laboratory under Contract DE-AC52-07NA27344.
† clark245@llnl.gov

ISBN: 978-3-95450-232-5 ISSN: 2673-7000 doi:10.18429/JACoW-NAPAC2022-TUZE4

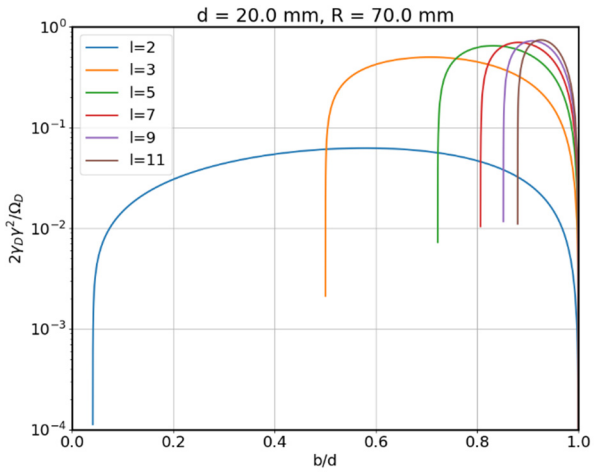

Figure 1: shows the analytical growth rate computed in the case of a uniform density electron annulus with a beampipe radius R=74.09 mm and a) beam outer radius d = 10 mm and b) d = 40 mm.

radii d, (not shown) the low mode number (l=2) growth rate decreases significantly, however the higher order modes tend to stay constant. In the limit of taking the enclosed axial magnetic flux in the beam to be conserved, which is an adiabatic invariant, then as the beam adiabatically contracts with increasing B, and the diocotron frequency should remain constant in that adiabatic limit.

This implies that the geometric factor for a weakly unstable beam with a wide annulus and limited size core of b/d < 0.5 will be diminished when moving to smaller beam size. The adiabatic invariance is clearly broken though as the characteristic length scale of variation in the axial magnetic field strength is typically on the order of or smaller than the betatron wavelength of the beam, so this is a weak statement that is meant to give some under-standing of what the geometric factors imply in this case. It should also be noted that the assumption of $\frac{\omega_{pe}^2}{\omega_{ce}^2} \ll 1$, used in deriving the drift-Poisson model which is used to calculate these growth rates is broken in many instances with high current beams. This makes it imperative that we look at accelerator simulations to assess the impact on the beam of instability driven by ring distributions.

The growth rate in Eq. (1) gives us some sense of the geometric factor that is multiplied into the maximal growth rate for the diocotron instability and a bound for how large the density hole in the beam can be before it goes unstable. Generally, the instability for mode l >2 is suppressed if the beam density only has concavity within the inner 1/2 of the beam. The l=2 mode, which is a squashing mode has a small geometric factor and should not grow much so long as the beam is relatively uniform in the outer half of the beam (b/d > 0.5).

Simulations of drifting beam profiles at various energies and profiles were performed to get a feel for how the instability grows and saturates, which is quite similar to simulation work done previously. [16-17] The key characteristics are that the beam must have shear to try to remain at a constant radius in a drift section with constant magnetic field, which will drive the current layer to form vortices and broaden. Since the growth falls off quickly as the layer broadens and b/d gets smaller, the instability will saturate quickly. It was observed in simple drift simulations that it requires ~5 e-folds for the instability to broaden enough to see measurable emittance growth in the beam. Additionally, since the growth rate scales like $1/\gamma^2$ and in the adiabatic limit, the diocotron frequency $\Omega_D \propto n_e/B_z$ will remain constant, then the beam will be much more susceptible to diocotron growth when it is larger, and less energetic. In an accelerator, the beam will not be moving adiabatically, the particle distribution will not have the same shear profile as the beam in which each particle stays at the same radius, and it will be undergoing constant focusing and expansion as it propagates through the machine. It is for these reasons that it is important to look at how the beam delivered and accelerated behaves in high fidelity simulations which can resolve azimuthal electric fields.

WARP XY-SLICE SIMULATIONS OF THE SCORPIUS ACCELERATOR

This section will apply the Warp XY-slice model to the problem of transporting a beam from cathode to target in the Scorpius accelerator to assess the impact of diocotron instability growth. The simulation presented uses a nominal tune[10] that was adapted to the current version of the accelerator design. The slice simulations are initialized in the AK gap at 0.5 m. The slice simulations use roughly 2 million macro-particles and have transverse cell dimension of 0.25 mm to be able to appropriately resolve the growing azimuthal modes for a beam with an envelope radius ~5 mm.

The RMS beam radius for the magnetic field tune shown in Fig. 2 matches well with the 1D slice code Amber, however it shows a touch more oscillation in the RMS beam radius. In general, the beam focuses down quickly and stays focused through the bulk of the machine. This is done primarily to stabilize the beam breakup instability. It incidentally also suppresses diocotron growth, however the rapid focusing could contribute to non-linear focusing effects that put the beam into an unstable configuration.

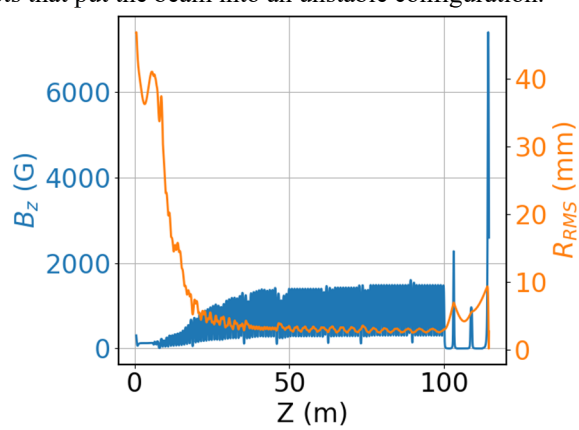

Figure 2: shows the axial magnetic field on axis (blue) and the beam RMS radius along the length of the machine.

ISBN: 978-3-95450-232-5 ISSN: 2673-7000 doi:10.18429/JACoW-NAPAC2022-TUZE4

Figure 3 shows that for maximally unstable beams, the e-folding length for an unstable configuration is about 10 m, which is much less than the machine length. The emittance growth between 20-30 m matches with what we expect given an unstable current density profile. It is observed however that the emittance growth is not extremely large, and it appears to saturate quickly and shut off as the beam energy increases.

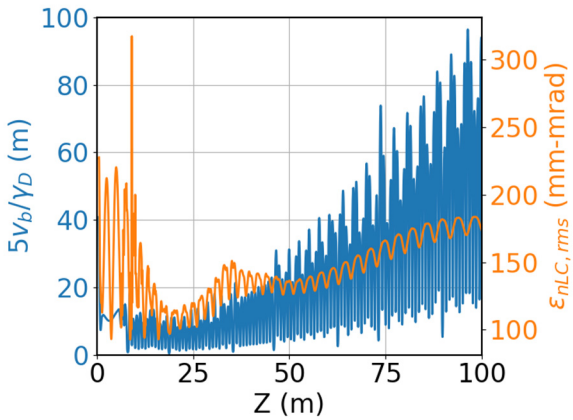

Figure 3: shows the 5 e-fold growth length (blue) and the beam Lapostolle Lee-Cooper emittance along the length of the machine.

Figure 4 shows a progression of the coalescence of modes into the slower growing lower mode numbers. Figure 4c shows the tell-tale vortices that are a feature of the saturation of the diocotron instability. The beam at the end of the accelerator has mixed around and contains some current density hot spots. These hotspots and azimuthal mode structure could potentially show up in radiographs, however the results would need to be coupled into a target simulation to determine the potential impact of the beam structure.

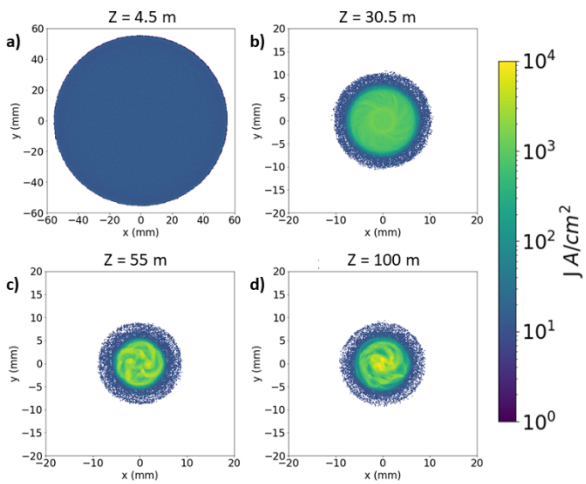

Figure 4: shows the beam in configuration space at (a) 4.5 m in the injector, (b) at 30 m after initial saturation, at (c) 55 m showing coalescence of higher modes to lower modes, and (d) at the accelerator exit at 100 m.

The overall results show manageable emittance growth during the saturation phase of the diocotron instability. The beam transports through the accelerator and does not experience catastrophic beam loss or emittance growth that would bring the beam out of specification to satisfy the radiographic requirements.

CONCLUSION

The newly developed Warp XY-slice solver was used to analyse the growth of the diocotron modes during transport through the accelerator and determine that the final design for the machine is sufficient to suppress significant diocotron instability growth and emittance growth. The XY-slice simulations suggest that the tuned machine should deliver a beam of sufficient quality for radiography measurements.

Future work on this topic could include modelling of FXR or DARHT beams and comparing to suspected radiographs that show possible azimuthal structure. Possible experiments putting the tune into a regime of increased diocotron growth could be examined against simulation results to validate the models. The beam model can also be integrated into target models to examine the interactions of beams that exhibit modal structure with the target to determine the impact on radiographic quality.

DISCLAIMER

REFERENCES

[1] B. Kulke, T. S. Innes, R. Kihara, and R. D. Scarpetti, "Initial Performance Parameters on FXR," Baltimore, MD, USA, UCRL-87306, CONF-820626-6, Jun. 1982, p. 6.

[2] M. Ong, C. Avalle, R. Richardson, and J. Zentler, "LLNL flash X-ray radiography machine (FXR) double-pulse upgrade diagnostics," *Digest of Technical Papers, 11th IEEE International Pulsed Power Conference (Cat. No. 97CH36127)*, Baltimore, MA, USA, 1997, vol. 1, pp. 430-435. doi:10.1109/PPC.1997.679369

ISBN: 978-3-95450-232-5 ISSN: 2673-7000 doi:10.18429/JACoW-NAPAC2022-TUZE4

[3] L. G. Multhauf, N. L. Back, L. F. Simmons, J.-M. Zentler, and R. D. Scarpetti, "The LLNL flash x-ray induction linear accelerator (FXR)," in *Proc. SPIE 4948, 25th International Congress on High-Speed Photography and Photonics*, Beaune, Finland, Jul. 2003, p. 622. doi:10.1117/12.516922

[4] R. D. Scarpetti, J. K. Boyd, G. G. Earley, K. L. Griffin, R. G. Ken, and R. Kihara, "Upgrades to the LLNL Flash X-Ray Induction Linear Accelerator (FXR)," *Digest of Technical Papers. 11th IEEE International Pulsed Power Conference (Cat. No. 97CH36127)*, Baltimore, MA, USA, 1997, p. 6. doi:10.1109/PPC.1997.679405

[5] C. Ekdahl *et al.*, "Initial electron-beam results from the DARHT-II linear induction accelerator," *IEEE Trans. Plasma Sci.*, vol. 33, no. 2, pp. 892–900, Apr. 2005. doi:10.1109/TPS.2005.845115

[6] Y. Chen *et al.*, "Scaled Accelerator Test For the DARHT-II Downstream Transport System," in *Proc. 2005 IEEE Pulsed Power Conference*, Monterey, CA, Jun. 2005, pp. 789–792. doi: 10.1109/PPC.2005.300779

[7] M. Crawford and J. Barraza, "Scorpius: The Development of a New Multi-Pulse Radiographic System," in *Proc. 2017 IEEE 21st International Conference on Pulsed Power (PPC) 2017*, pp. 1-6. doi:10.1109/PPC.2017.8291266

[8] E. Henestroza, "Sensitivity Analysis of the DARHT-II 2.5MV/2kA Diode," Lawrence Berkeley National Lab., Berkeley, CA, LBNL--62296, HIFAN 1562, 928866, Dec. 2006. doi:10.2172/928866

[9] C. Ekdahl *et al.*, "Emittance Growth in the DARHT-II Linear Induction Accelerator," *IEEE Trans. Plasma Sci.*, vol. 45, no. 11, pp. 2962–2973, Nov. 2017. doi:10.1109/TPS.2017.2755861

[10] C. Ekdahl, "Cathode to Target Simulations for Scorpius: I. Simulation Codes and Models," Los Alamos National Lab., Los Alamos, NM, LA-UR-21-21022, 2021.

[11] C. Ekdahl, "Beam Envelope Stability in an Advanced Linear Induction Accelerator," *IEEE Trans. Plasma Sci.*, vol. 49, no. 10, pp. 3092–3098, Oct. 2021. doi:10.1109/TPS.2021.3112511

[12] S. E. Clark, W. D. Stem, C. N. Melton, N. Pogue, and J. Ellsworth, "Three-Dimensional Particle-in-Cell Analysis of Mechanical Design Tolerances of the Scorpius Injector With Warp," *IEEE Trans. Plasma Sci.*, vol. 50, no. 7, pp. 2068–2077, Jul. 2022. doi:10.1109/TPS.2022.3181566

[13] J. H. Yu and C. F. Driscoll, "Diocotron wave echoes in a pure electron plasma," *IEEE Trans. Plasma Sci.*, vol. 30, no. 1, pp. 24–25, Feb. 2002. doi:10.1109/TPS.2002.1003905

[14] C. F. Driscoll, "Observation of an unstable *l=1* diocotron mode on a hollow electron column," *Phys. Rev. Lett.*, vol. 64, no. 6, pp. 645–648, Feb. 1990. doi:10.1103/PhysRevLett.64.645

[15] R. H. Levy, "Diocotron Instability in a Cylindrical Geometry," *Phys. Fluids*, vol. 8, no. 7, p. 1288, 1965. doi:10.1063/1.1761400

[16] Y. H. Jo, J. S. Kim, G. Stancari, M. Chung, and H. J. Lee, "Control of the diocotron instability of a hollow electron beam with periodic dipole magnets," *Phys. Plasma*, vol. 25, no. 1, p. 011607, Jan. 2018. doi:10.1063/1.5018425

[17] V. V. Mikhailenko, J. Seok Kim, Y. Jo, V. S. Mikhailenko, and H. June Lee, "Non-modal analysis of the diocotron instability for cylindrical geometry with conducting boundary," *Phys. Plasma*, vol. 21, no. 5, p. 052105, May 2014. doi: 10.1063/1.4875341